Surgical and Radiologic Anatomy (2019) 41:75–85
https://doi.org/10.1007/s00276-018-2134-x

ORIGINAL ARTICLE

Fibular groove morphology and measurements on MRI: correlation with fibularis tendon abnormalities

George R. Matcuk Jr.[1] · Dakshesh B. Patel[1] · Steven Cen[1] · K. Soraya Heidari[2] · Eric W. Tan[3]

Received: 7 June 2018 / Accepted: 1 November 2018 / Published online: 8 November 2018

Abstract

Purpose Fibular (peroneal) groove morphology may influence fibularis tendon pathology, including tendinosis, tears, and luxation. The study goal was to evaluate the inter-reader agreement of morphologic characterization and measures of the fibular groove at two different levels on MRI and correlation with fibularis tendon pathology.

Materials and methods 47 ankle MRIs in patients without lateral ankle pain were reviewed by two musculoskeletal radiologists. Fibular groove morphology and various measurements were assessed at both the level of the tibial plafond and 1 cm proximal to the tip of the lateral malleolus. Fibularis tendon pathology and other variants were also recorded. Intraclass correlation (ICC) and kappa statistic (κ) were applied to assess inter-observer agreement. Receiver operating characteristic (ROC) and area under the curve (AUC) analysis were performed to determine correlation between fibular groove morphometry and fibularis (peroneus) brevis tendon tears.

Results Between readers, there was fair-to-excellent agreement (ICC = 0.61–0.95) for performed fibular groove measurements and moderate-to-very good agreement for identification and description of fibular groove and fibularis tendon morphology and pathology and normal variants in this region (κ = 0.46-1), with the exception of fibular groove morphology at 1 cm proximal to the lateral malleolar tip (κ = 0.34). Individually, no measurement or description of pathology could discriminate between patients with or without fibularis brevis tendon tears except fibularis brevis tendinosis (AUC = 0.87 for reader 1).

Conclusion There is overall moderate-to-excellent inter-reader agreement for various measurements and descriptors of fibular groove and fibularis tendon morphometry and pathology, including novel measurements introduced in this study.

Keywords Imaging · Magnetic resonance · Ankle · Fibula · Morphology · Anatomy

Introduction

The fibularis (peroneus) longus and brevis are the primary muscles responsible for foot eversion [6]. The fibularis tendons also serve as dynamic stabilizers of the lateral ankle. Fibularis tendon disorders including tendinosis, tear, and subluxation/dislocation are commonly caused by acute trauma, overuse, and inflammation [19, 22]. Anatomic variants may also predispose patients to fibularis tendon disorders [18, 25], including morphologic abnormalities of the retromalleolar fibular (peroneal) groove [10, 14, 15], enlarged fibular (peroneal) tubercle (or trochlea) of the calcaneus [2], the presence of a low-lying fibularis brevis muscle belly [7–9], or fibularis (peroneus) quartus accessory muscle [3, 26].

In particular, studies have indicated that a convex, irregular, or even flat fibular groove may predispose individuals to fibularis tendon dislocation and tendon irritation and longitudinal tears, although these morphologies may be seen in more than two-thirds of asymptomatic ankles [18]. Low-lying fibularis brevis and fibularis quartus muscle bellies may cause a mass-effect, or crowding of the retromalleolar space and predispose to fibularis tendon pathology and

IRB: This study was approved by the USC institutional review board.

✉ George R. Matcuk Jr.
matcuk@usc.edu

[1] Department of Radiology, Keck School of Medicine, University of Southern California, 1520 San Pablo Street, Suite L1600, Los Angeles, CA 90033, USA

[2] Keck School of Medicine, University of Southern California, Los Angeles, CA, USA

[3] Department of Orthopaedic Surgery, University of Southern California, Los Angeles, CA, USA

superior fibular (peroneal) retinaculum injuries [7, 25, 26]. Furthermore, enlarged fibular tubercles or retrotrochlear eminences may lead to fibularis (peroneal) tenosynovitis and tendon irritation [2].

The morphology of the fibular groove and these anatomic variants are important to the foot and ankle surgeon as each of these features may result in fibularis tendon instability and pain. In cases of acute and chronic fibularis tendon subluxation/dislocation, open or percutaneous deepening of the groove, debridement/repair/reconstruction of the fibularis tendons, and/or repair of the superior fibular retinaculum can provide good outcomes [4, 23, 24]. However, how much each of these individual factors affects fibularis tendon pathology remains unknown.

The goal of this study is to provide normal ranges for fibular groove morphometric measurements, including new measurements devised for this study, and highlight the incidence of fibularis tendon shapes and pathology and lateral ankle variants in patients without lateral ankle pain. This study will also assess the inter-reader variability for each of these measurements and findings. Finally, these results will be analyzed to identify potential associations with fibularis brevis tears.

Materials and methods

Following institutional review board approval, MRI examinations of the ankle without a clinical history of lateral ankle pain or suspected fibularis tendon pathology were retrospectively identified from a search of radiology reports from May to November 2016. This list was then manually vetted to include examinations on a 3T MRI scanner and clinical indications and histories were evaluated to exclude studies with lateral ankle pain. This resulted in a list of 49 ankle MRIs. One examination was excluded from this study, as it was protocoled for evaluation for osteomyelitis and was limited by motion artifact. Another examination was excluded as it was performed on a 12-year-old skeletally immature female, which was below our inclusion criteria of patients 18 years of age or older. Other exclusion criteria included a history of ankle fracture or dislocation, previous lateral ankle surgery, or MRI obtained at an outside institution.

The remaining 47 ankle MRI examinations were included in our study. The indications included non-lateral ankle or foot pain in 27 (57%); injury or sprain in seven (15%); concern for posterior tibial tendon pathology in four (9%), Achilles pathology in three (6%), or infection in three (6%); and mass evaluation in three (6%) patients. The ankle MRIs were obtained on a 3T scanner with the following pulse sequences: axial proton density (PD) and PD fat saturation (FS); sagittal T1 and short tau inversion recovery (STIR); coronal T1 and PD FS; images at 2.5–3 mm slice thickness with a 0.5 mm interslice gap.

Each of these examinations was review by two academic attending musculoskeletal radiologists (G.M. and D.P.) with 8 and 10 years of experience, respectively. Evaluation of fibular groove morphology and measurements were performed on axial MR images at each of two levels: first at the level of the tibial plafond and syndesmotic ligaments and the second 1 cm proximal to the tip of the lateral malleolus (Fig. 1). In order to more accurately assess variability of these measurements in a practice-like setting, the axial images for each level were recorded by each radiologist, but not agreed upon before each set of measurements were performed.

Fibular groove morphology was classified as either concave, convex, irregular (undulating), or flat (Fig. 2), as initially discussed by Rosenberg et al. and similarly used by Wang et al. and Galli et al. [6, 16, 25]. The length and depth (positive if convex, negative if concave, and 0 if flat) of the fibular groove were measured at each level (Fig. 3). Several other novel measurements were developed for this study, including a bowing ratio (depth divided by length times 100%); angle of the fibular groove relative to the bimalleolar axis (Fig. 4); area and circumference of the lateral (peroneal) compartment (bounded by the fibula anteriorly, superior fibular retinaculum laterally, and adjoining fascia posteriorly and medially) (Fig. 5). The goal of the bowing ratio is to identify a more objective and quantitative measurement of the degree of concavity or convexity of the fibular groove. The angle of the fibular groove relative to the bimalleolar axis is proposed to quantitate the degree of tilt or slope of the fibular groove. The area and circumference measurements are proposed to offer a quantitative assessment of the size and potentially the degree of crowding of the lateral compartment at these levels. If an osteophyte was present at the fibular origin of the superior fibular retinaculum, the size (in mm) was also measured.

For each ankle, blinded review of fibularis brevis and fibularis longus tendon pathology was also performed by each reviewer. Morphology was described as one of the following shapes: round, boomerang (i.e., curved or crescentic), or flat. Tendinopathy was graded as none, mild, moderate, or severe based on qualitative assessment on increased intrasubstance signal intensity on fluid-sensitive sequences. Tears were described as none, partial thickness, split (full thickness), or complete (rupture). Consensus review was performed for discrepant results for tears between the two readers. Tenosynovitis was graded as none, mild, moderate, or severe. Luxation was described as none, subluxated (partially lateral to the lateral aspect of the fibular groove), or dislocated (lateral and anterior to the fibular groove).

Reviewers also assessed each ankle for superior fibular retinaculum injury using Oden's surgical classification: normal, type I (pouch), type II (avulsion), type III (avulsion

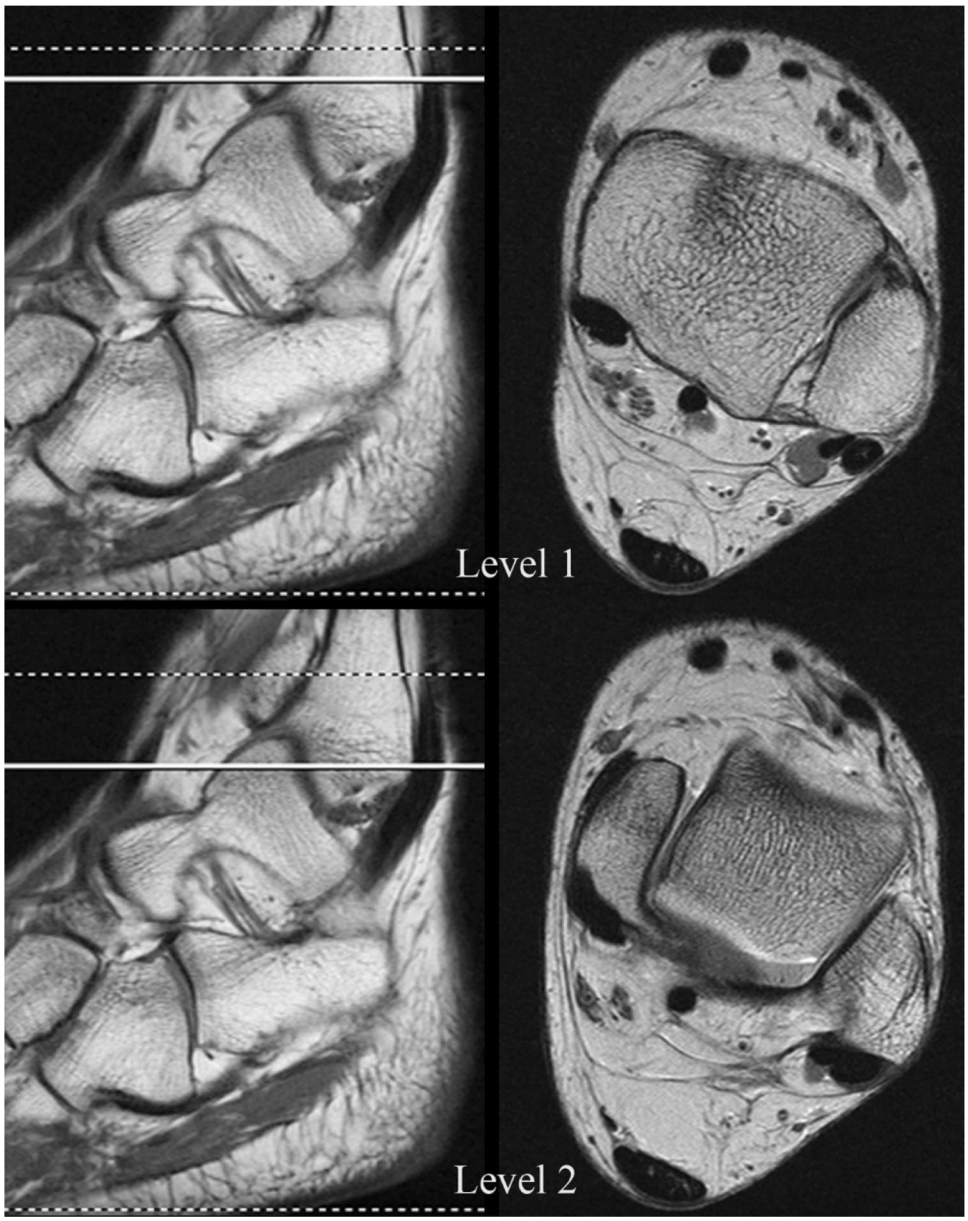

Fig. 1 Sagittal T1 (left, with solid white localizer lines, and dashed lines indicating the uppermost and lowermost imaged sections) and axial proton density (PD) (right) MR images of the ankle demonstrate the levels at which each fibular groove measurement was performed. Level 1 is at the level of the tibial plafond and syndesmotic ligaments. Level 2 is 1 cm proximal to the lateral malleolar tip

fracture), or type IV (tear) [13]. The fibular tubercle and retrotrochlear eminence were also measured as the maximum perpendicular distance (size or height in mm) from the lateral cortex of the calcaneus (Fig. 6). The presence or absence of a low-lying fibularis brevis muscle belly (defined as extending distal to the lateral malleolar tip), fibularis quartus accessory muscle, and os peroneum were also recorded for each patient.

The inter-reader agreement for continuous measurements was evaluated using intraclass correlation (ICC; two-way mixed with absolute agreement) and categorical measurements were evaluated with the kappa coefficient (κ). We used ICC cut-off values of < 0.40 = poor, 0.40–0.59 = fair, 0.60–0.74 = good, and > 0.74 = excellent agreement. We used κ cut-off values of < 0.20 = poor, 0.20–0.39 = fair, 0.40–0.59 = moderate, 0.60–0.80 = good, and > 0.80 = very good agreement. Inter-reader agreement for the axial image number selected to perform each of the described measurements was also assessed with kappa statistics, as well as the effect on the agreement for each measurement when the readers agreed or disagreed on which axial image to perform these measurements.

Receiver operating characteristic (ROC) and area under the curve (AUC) analysis were performed to determine correlation between fibular groove morphometry and fibularis brevis tendon tears. We used AUC cut-off values of < 0.60 = very poor, 0.60–0.69 = poor, 0.70–0.79 = fair, 0.80–0.90 = good, and > 0.90 = excellent accuracy.

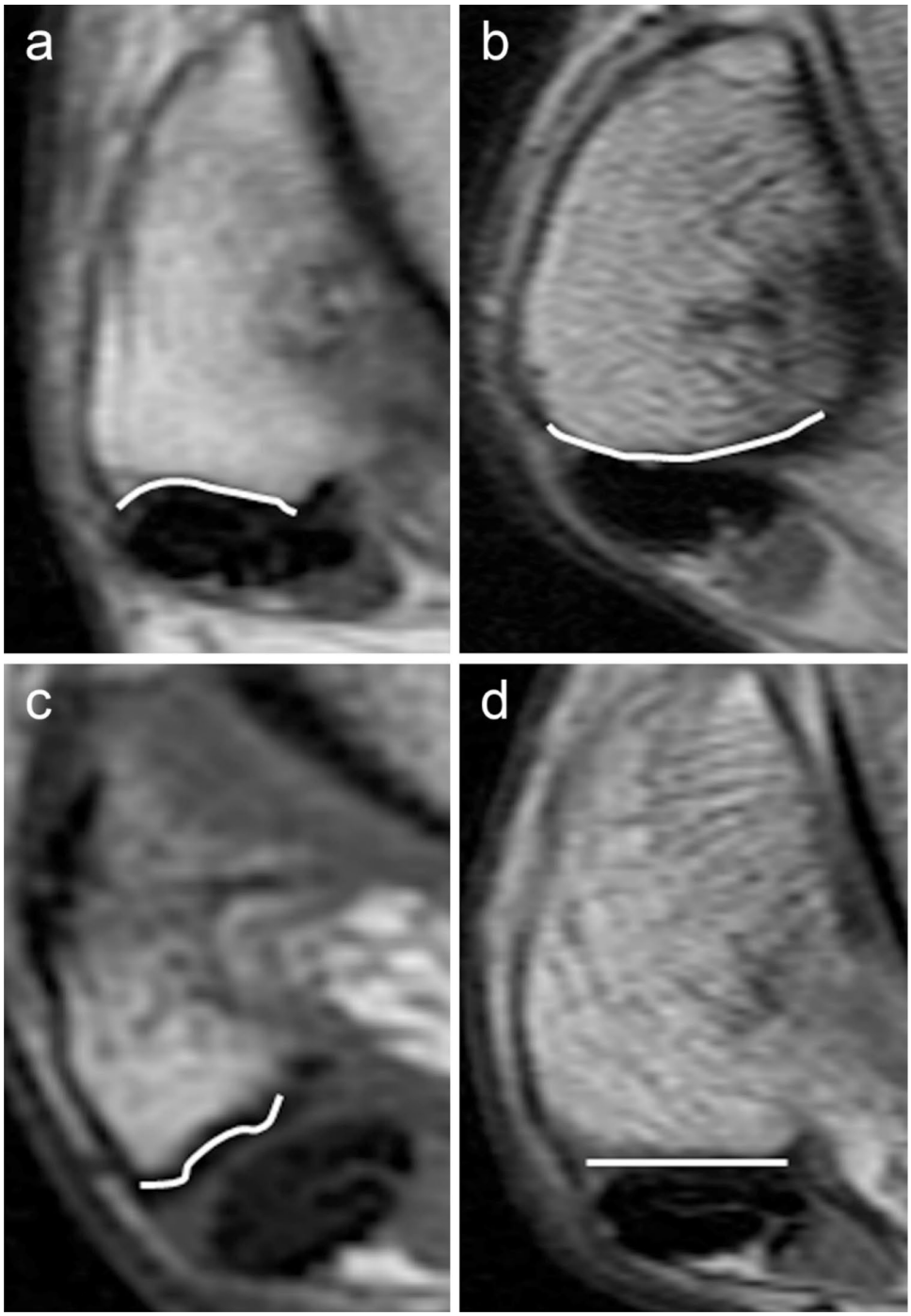

Fig. 2 Axial PD MR images with examples of each fibular groove morphological category: **a** concave, **b** convex, **c** irregular or undulating, and **d** flat

Results

Of the 47 ankle MRI examinations, two were opposite ankles (right and left) performed on the same patient on the same day. The age range of the patients was 19- to 79-years old with a mean age of 50 years old. There were 21 male patients and 25 female patients (the patient with both ankles imaged was female); 25 of the examinations were of the right ankle and the remaining 22 were of the left ankle.

Measurements of the fibular groove at each level (level 1 at the tibial plafond and level 2 at 1 cm proximal to the tip of the lateral malleolus) and of the fibular tubercle and retrotrochlear eminence are summarized in Table 1. Superior fibular retinaculum injury or fibularis tendon subluxation was not identified for any of these patients by either reader. In addition, osteophytes were rarely present at the superior fibular retinaculum origin at level 1 (only noted in three patients (6%) by reader 1 and six patients

Fig. 3 Axial PD MR image demonstrates measurements of the length (17.43 mm) and depth (2.8 mm) of the fibular groove 1 cm proximal to the lateral malleolar tip. From these measurements, a bowing ratio was also calculated as (depth ÷ length) × 100% (16% in this case)

Fig. 4 Axial PD MR image demonstrates measurement of the angle (arrow, 24°) of the fibular groove (black line) relative to the bimalleolar axis (white line)

Fig. 5 Axial PD MR image demonstrates measurement of the lateral compartment circumference (white line, 51 mm) and area (149 mm^2) bounded by the fibular groove, superior fibular retinaculum, and surrounding fascia

(13%) by reader 2) but were more common at level 2 (22 (47%) and 26 (55%) of patients noted by reader 1 and 2, respectively). Furthermore, no fibular tubercle was identified in 26 (55%) and 28 (66%) patients by reader 1 and 2, respectively. There was 100% agreement, except for the two additional cases identified by reader 1, with heights of 0.6 and 1.2 mm. A measurable retrotrochlear eminence was present in all patients, except in one patient where this was measured as 1.8 mm in height by reader 1 but not identified by reader 2.

Inter-reader reliability for each of these measurements was assessed using intraclass correlation (ICC) and presented in Table 2. At level 1, the readers performed their measurements on the same axial image number in 33/47 cases (70%). At level 2, the readers performed their measurements on the same axial image number in 34/47 cases (72%). For the cases where the readers chose to perform their measurements at different slice levels, the axial image chosen was only one slice above or below the image chosen by the other reader for all cases at level 1 and for 11 of the 13 cases at level 2, with only two of the cases at level 2 differing by two slice numbers. Agreement was almost always better when the readers performed their measurements on

Fig. 6 Axial PD MR image demonstrates measurement of the fibular tubercle (thin arrow, 4.5 mm) and retrotrochlear eminence (arrowhead, 5.2 mm) as the perpendicular distances relative to a line parallel to the lateral cortex. The fibularis brevis (thick arrow) and fibularis longus (curved arrow) tendons are separated by the fibular tubercle

the same axial image and worse when they performed their measurements on different axial images.

Reader 1 described no osteophyte present at the superior fibular retinaculum origin in 44 (94%) of cases at level 1 and in 25 (53%) of cases at level 2. Reader 2 described no osteophyte present at the superior fibular retinaculum origin in 41 (87%) of cases at level 1 and in 21 (45%) of cases at level 2. Inter-reader agreement for osteophyte size was only fair at both levels. Inter-reader agreement for fibular tubercle size was excellent (ICC = 0.90) and good for measurement of the size of the retrotrochlear eminence (ICC = 0.67).

Inter-reader reliability for categorization of fibular groove morphology, fibularis tendon and superior fibular retinaculum pathology, and for normal variants (low-lying fibularis brevis muscle belly, fibularis quartus accessory muscle, and os peroneum) was assessed using the kappa (κ) statistic (Table 3). For fibular groove morphology, reader 1 characterized the groove as concave in two (4%), convex in 16 (34%), irregular in one (2%), and flat in 28 (60%) cases at level 1 and concave in 11 (23%), convex in six (13%), irregular in 11 (23%), and flat in 19 (40%) cases at level 2. Reader 2 classified the fibular groove morphology as concave in two (4%), convex in 25 (53%), irregular in two (4%), and flat in 18 (38%) cases at level 1 and concave in 14 (30%), convex in 11 (23%), irregular in 12 (26%), and flat in 10 (21%) cases at level 2. Inter-reader agreement for characterization of fibular groove morphology was moderate at level 1, regardless of whether the readers used the same image for evaluation or not. However, at level 2, agreement was moderate when the readers used the same image, but poor when they used different axial images for evaluation.

There was good agreement for characterization of fibularis longus tendon shape ($\kappa = 0.71$) between readers, with agreement in 44 (94%) cases, with the vast majority described as round by both readers. For the discrepant cases, two were described as flat by one reader and round by the other and one was described as boomerang-shaped by one reader and round by the other. However, there was only moderate agreement ($\kappa = 0.50$) for fibularis brevis shape between readers, with more varied characterization. The fibularis brevis shape was classified as round in 17 (36%), boomerang in 17 (36%), and flat in 13 (28%) cases by reader 1 and round in 14 (30%), boomerang in 19 (40%), and flat in 14 (30%) cases by reader 2, with agreement between reader in only 32 (68%) cases.

Table 1 Measurements of fibular groove at each level and the fibular tubercle and retrotrochlear eminence by each reader

Measurement	Reader 1 Level 1	Reader 1 Level 2	Reader 2 Level 1	Reader 2 Level 2
Length (mm)	11.9 ± 2.2 (7–18)	10 ± 2.4 (6–17)	11.3 ± 2.7 (5.7–18.1)	10.6 ± 2.8 (5.8–16.9)
Depth (mm)	0.4 ± 0.8 (− 0.8–2.1)	0.1 ± 0.7 (− 1.5–2)	0.7 ± 0.9 (− 0.9–2.6)	0.7 ± 1.1 (− 3.6–2.2)
Bowing ratio (%)	3.8 ± 6.4 (− 5.8–19.1)	0.3 ± 7.1 (− 15–17.9)	6 ± 7.1 (− 8–20)	0.7 ± 9.4 (− 19–19)
Angle relative to the bimalleolar axis (°)	34 ± 9 (14–50)	13 ± 11 (− 11–36)	35 ± 9 (11–51)	17 ± 12 (− 10–37)
Lateral compartment area (mm^2)	144 ± 41 (73–256)	124 ± 34 (65–239)	146 ± 40 (77–245)	112 ± 35 (46–251)
Lateral compartment circumference (mm)	52 ± 7 (39–66)	50 ± 7 (36–69)	53 ± 7 (40–68)	51 ± 9 (30–75)
Osteophyte size (mm) (when present)	1.1 ± 0.3 (0.9–1.3)	1.5 ± 0.6 (0.7–3)	1.3 ± 0.3 (1.0–1.8)	1.6 ± 0.6 (0.6–2.8)
Fibular tubercle (mm) (when present)	2.7 ± 1.6 (0.6–7.6)	3.8 ± 1.5 (0–7.2)		
Retrotrochlear eminence (mm)	3 ± 1.2 (1.4–6.7)	3.8 ± 1.5 (1.6–7.4)		

Measurements presented as mean ± standard deviation and range (low–high)

Table 2 Inter-reader agreement intraclass correlation (ICC), standard error of measurement (SEM), and minimal detectable change (MDC) values of fibular groove measurements at each level and changes when the same or a different axial image was selected

Measurement	All			Same axial image number			Different axial image number		
	ICC	SEM	MDC	ICC	SEM	MDC	ICC	SEM	MDC
Level 1									
Axial image number	0.99	0.36	1	1	0	0	0.96	0.57	1.58
Length	0.76	1.32	3.66	0.80	1.15	3.19	0.70	1.63	4.52
Depth	0.73	0.45	1.25	0.82	0.38	1.05	0.45	0.58	1.61
Bowing ratio	0.76	3.49	9.67	0.82	3.21	8.9	0.51	3.95	10.95
Angle relative to the bimalleolar axis	0.68	5.71	15.83	0.71	6.05	16.77	0.6	4.42	12.25
Lateral compartment area	0.95	8.82	24.45	0.96	8.61	23.87	0.94	9.72	26.94
Lateral compartment circumference	0.84	2.76	7.65	0.82	2.93	8.12	0.89	2.28	6.32
Osteophyte size	0.50	0.33	0.91	0.76	0.16	0.44	0.32	0.56	1.55
Level 2									
Axial image number	0.99	0.46	1.28	1	0	0	0.97	0.86	2.38
Length	0.61	1.75	4.85	0.76	1.39	3.85	0.24	2.46	6.82
Depth	0.61	0.72	2	0.59	0.73	2.02	0.59	0.71	1.97
Bowing ratio	0.62	5.79	16.05	0.57	5.50	15.25	0.64	6.80	18.85
Angle relative to the bimalleolar axis	0.73	6.07	16.83	0.78	5.27	14.61	0.62	7.85	21.76
Lateral compartment area	0.87	12.57	34.84	0.78	12.61	34.95	0.94	12.31	34.12
Lateral compartment circumference	0.72	4.82	13.36	0.71	4.66	12.92	0.73	5.45	15.11
Osteophyte size	0.41	0.70	1.94	0.46	0.68	1.88	0.28	0.73	2.02
Fibular tubercle	0.90	0.64	1.77						
Retrotrochlear eminence	0.67	0.78	2.16						

ICC < 0.40 = poor, 0.40–0.59 = fair, 0.60–0.74 = good, and > 0.74 = excellent agreement

Table 3 Inter-reader agreement kappa (κ) statistic values of fibular groove morphology, tendon and superior fibular retinaculum characteristics, and identification of normal variants

Measurement	All	Same axial image number	Different axial image number
Fibular groove morphology level 1	0.56	0.56	0.55
Fibular groove morphology level 2	0.34	0.50	0.11
Fibularis longus tendon shape	0.71		
Fibularis longus tendinosis	0.59		
Fibularis longus tendon tear	1		
Fibularis longus tendon luxation	1		
Fibularis brevis tendon shape	0.50		
Fibularis brevis tendinosis	0.59		
Fibularis brevis tendon tear	0.67		
Fibularis brevis tendon luxation	1		
Fibularis tenosynovitis	0.86		
Superior fibular retinaculum	1		
Low-lying fibularis brevis muscle belly	0.46		
Fibularis quartus	0.78		
Os peroneum	0.48		

κ < 0.20 = poor, 0.20–0.39 = fair, 0.40–0.59 = moderate, 0.60–0.80 = good, and > 0.80 = very good agreement

Fibularis tenosynovitis (fluid signal intensity within the fibularis tendon sheath) was identified in 15 (32%) patients by reader 1 and in 12 (26%) patients by reader 2. When present it was characterized as mild, with the exception of one case described as moderate by both readers. Reader 1 agreed with all cases described as having tenosynovitis by reader 2, although for three of the cases described as having tenosynovitis by reader 1, reader 2 described those

cases as having no tenosynovitis, although there was excellent agreement overall ($\kappa = 0.86$).

A low-lying fibularis brevis muscle belly was described as present in 5 (11%) cases by reader 1 and 3 (6%) cases by reader 2, however, there was only agreement for two of these cases between readers. A fibularis quartus muscle was identified in six (13%) cases by reader 1, with agreement for four (9%) of these cases by reader 2. An os peroneum was only identified in 2 (4%) of the patients by each reader, but with agreement between readers for only one of these cases.

Fibularis longus tendinosis was described in eight (17%) cases (seven mild, one moderate) by reader 1 and in 12 (26%) cases (all mild) by reader 2, with differing characterization between readers in 18 cases. Similarly, fibularis brevis tendinosis was described in 17 (36%) cases (12 mild, 5 moderate) by reader 1 and in 14 (30%) cases (11 mild, two moderate, one severe) by reader 2, with differing characterizations between readers in 12 cases. Overall inter-reader agreement for characterization of both fibularis longus and brevis tendinosis was moderate ($\kappa = 0.59$ for each).

There were no fibularis longus tears identified by either reader. For the fibularis brevis tendon, at initial assessment, six split and seven partial tears were identified by reader 1 and 11 split and two partial tears were identified by reader 2. There was disagreement for seven cases, which were then re-reviewed and classified by consensus. Two of the cases that were initially classified as partial tears by reader 1 were reclassified as tendinosis without tear and two cases that were classified as no tear by reader 1 were reclassified as split tears after consensus review. The remaining three cases were classified as partial tears by reader 1 and split tears by reader 2 and all were classified as partial tears after consensus review. Overall, there were 34 (72%) cases without fibularis brevis tear and 13 (28%) cases with tear (eight split and five partial tears) after consensus review.

Using this consensus data, receiver operating characteristics (ROC) curve analysis was performed and area under the curve (AUC) values calculated for each measurement at each level and each finding for each reader, as well as an average of each reader's measurements, with these values presented in Table 4. Although there was good discrimination for the presence or absence of fibularis brevis tear on the basis of the presence or absence of fibularis brevis tendinosis for reader 1 (AUC = 0.87), no other measurement or finding demonstrated good or better ability to differentiate these two groups on an individual basis. The sample size for this study was too small to apply more sophisticated techniques such as Classification and Regression Tree (CART) to identify a group of variables and cut-off values that could reliably discriminate between patients with or without a fibularis brevis tear.

Table 4 Receiver operating characteristic (ROC) curve analysis and area under the curve (AUC) values of each measurement or finding for discriminating between patients with or without fibularis brevis tears

Measurement	Reader 1	Reader 2	Average
Level 1			
Length	0.48	0.50	0.50
Depth	0.51	0.51	0.53
Bowing ratio	0.52	0.52	0.55
Angle relative to the bimalleolar axis	0.71	0.65	0.66
Lateral compartment area	0.54	0.57	0.55
Lateral compartment circumference	0.68	0.63	0.64
Osteophyte size	0.51	0.57	0.57
Level 2			
Length	0.56	0.61	0.60
Depth	0.50	0.51	0.48
Bowing ratio	0.50	0.53	0.46
Angle relative to the bimalleolar axis	0.67	0.58	0.62
Lateral compartment area	0.58	0.66	0.63
Lateral compartment circumference	0.61	0.70	0.65
Osteophyte size	0.52	0.50	0.52
Fibular tubercle	0.46	0.49	0.47
Retrotrochlear eminence	0.77	0.71	0.76
Finding			
Fibular groove morphology level 1	0.57	0.61	
Fibular groove morphology level 2	0.54	0.52	
Fibularis longus tendon shape	0.51	0.53	
Fibularis longus tendinosis	0.54	0.54	
Fibularis brevis tendon shape	0.56	0.61	
Fibularis brevis tendinosis	0.87	0.64	
Fibularis tenosynovitis	0.51	0.52	
Low-lying fibularis brevis muscle belly	0.59	0.56	
Fibularis quartus	0.54	0.51	
Os peroneum	0.52	0.53	

AUC < 0.60 = very poor, 0.60–0.69 = poor, 0.70–0.79 = fair, 0.80–0.90 = good, and > 0.90 = excellent accuracy

Discussion

This study provides a range of values of fibular groove, fibular tubercle, and retrotrochlear measurements (Table 1) that may serve as a useful normal reference for future studies that evaluate fibular groove morphometry and its association with fibularis tendon pathology and lateral ankle pain. Furthermore, this study shows that there is moderate-to-very good agreement between readers for these measurements (Table 2), indicating that reproducibility should be relatively good between studies.

As expected, agreement was almost always better when the readers performed their measurements on the same axial image and worse when they were performed their measurements on different axial images. However, large drop-offs in agreement were only seen for fibular groove depth and bowing ratio at level 1 (at the level of the tibial plafond), fibular groove length and morphologic characterization at level 2 (1 cm proximal to the lateral malleolar tip), and osteophyte size at both levels, when these measurements were not performed on the same axial images. The decreased agreement for these measurements indicates that there are probably significant changes in these morphometric features over short distances at these levels and that caution should be applied when generalizing the reproducibility of these particular measurements in future studies, especially if stringent criteria for the exact position of measurement are not applied.

Inter-reader agreement for identification and characterization of fibularis tendon shape and pathology ranges from moderate to very good (Table 3). Agreement is better for fibularis longus shape (where the tendon was almost always characterized as round by both readers) than for fibularis brevis shape, where the characterization was more evenly divided between round, boomerang, and flat shapes and where the distinction between boomerang and flat is not always clear.

It is important to note that in this patient cohort without reported symptoms of lateral ankle pain, no injuries to the superior fibular retinaculum or fibularis tendon subluxations or dislocations were identified. In addition, no tears of the fibularis longus tendon were identified. Conversely, there was a significant minority of patients with imaging evidence of fibularis tenosynovitis (26–32%), fibularis longus (17–26%) or brevis (30–36%) tendinosis, and fibularis brevis tears (28%). These findings concur with a study by O'Neil et al., which demonstrated fibularis tendon pathology in 35% of routine ankle MRIs in asymptomatic individuals [12]. The incidence of tendinosis was also similar to a study of MRI of asymptomatic lateral ankles by Galli et al., which also had no examinations with fibularis longus tears, although our incidence of fibularis brevis tears was higher than the 2.8% observed in their study [6]. Inter-reader agreement was very good for characterization of fibularis tenosynovitis, good for fibularis brevis tears, but only moderate for tendinosis.

A low-lying fibularis brevis muscle belly was identified in 6–11% of patients in this study, and despite being considered a "rare anomaly", a study by Mirmiran et al. showed that the prevalence may be as high as 62% intraoperatively in patients with lateral ankle pain and is associated with tenosynovitis (29%), tendon subluxation (81%), and fibularis brevis tear (86%), although 94% of these reported low-lying fibularis brevis muscle bellies were not identified on preoperative MRI [11]. A fibularis quartus was identified in 9–13% of patients, which is in-line with the reported prevalence of 10% on ankle MRI, although lower than the reported incidence of 22% on ultrasound and 13–26% in cadaveric studies [20]. Although the fibularis quartus is a commonly encountered asymptomatic variant, it has also been associated with lateral ankle pain and instability as well as fibularis tenosynovitis, tendon subluxation, and tears. An os peroneum was identified in 4% of cases, which also corresponds to the reported incidence by radiography (4.7%) [5]. Although the os peroneum is a sesamoid of the fibularis longus tendon and considered a normal accessory ossicle, fracture or enlargement with entrapment at the cuboid tunnel can be associated with fibularis longus tears [21].

The identification of a retrotrochlear eminence in all patients (except one by reader 2) is consistent with the identification in 100% and 98% by Saupe et al. and Wang et al., respectively [18, 25]. A fibular tubercle was identified in 40–45% of patients in this study, which is within the reported prevalence range of 32–97% of prior studies [1, 17]. The average size and ranges of the fibular tubercle and retrotrochlear eminence measurements are also similar to those reported by Saupe et al. [18].

As would be expected, fibularis brevis tendinosis has a high correlation with fibularis brevis tears, with an AUC of 0.87 for ROC curve analysis. Although no single fibular groove measurements at either the level of the tibial plafond (level 1) or 1 cm proximal to the lateral malleolar tip (level 2) or other anatomic variant can reliably discriminate between patients with versus without fibularis brevis tears, larger retrotrochlear eminences did show fair discrimination (AUC above 0.7 for both readers), which may indicate a more important role in fibularis tendon pathology that should be investigated in future studies.

Limitations of this study include the small sample size of only 47 ankles, limiting the power of our conclusions and the ability to extract additional information regarding correlation of fibular groove morphometric measurements, lateral ankle variants, and fibularis tendon pathology. In addition, although the cohort in this study did not have reported lateral ankle pain, these patients did have other clinical indications for obtaining an ankle MRI, which may have masked lateral ankle symptoms. Therefore, this cohort may have a higher incidence of fibularis tenosynovitis, tendinosis and fibularis brevis tears than a group of age-matched healthy volunteers.

For future investigations, it would be useful to compare the measurements and findings in this group of patients without reported lateral ankle pain to a cohort of patients with lateral ankle pain and subsequent surgical follow-up. There may be some fibular groove morphometric measurements and other lateral ankle features that are significantly different and could potentially be correlated with fibularis tendon pathology if compared to such a group, particularly since the cohort in this study did not have any cases of superior fibular retinaculum injury, tendon subluxation or dislocation,

or fibularis longus tears. There was also no surgical correlation for any of the imaging findings discussed in this study.

In conclusion, this study helps to define the normal range of measurements of the fibular groove, including novel measurements introduced in this study, such as the bowing ratio and angle relative to the bimalleolar axis. This study also shows that patients may still present with imaging evidence of fibularis tenosynovitis, tendinosis, and even fibularis brevis tear, despite the absence of lateral ankle pain or symptoms. There is also overall moderate-to-excellent inter-reader agreement for these fibular groove measurements and for the identification and description of fibularis tendon pathology. Although no single measurement or finding was shown to accurately discriminate patients with or without fibularis brevis tears, further research in a larger group and comparison to patients with lateral ankle pain and fibularis tendon pathology may further elucidate morphologic features that predispose to these injuries.

Author Contributions All authors provided input for the manuscript writing/editing. Matcuk: project development, data collection, data analysis; Patel: project development, data collection, data analysis; Cen: data analysis; Heidari: project development, data collection; Tan: project development.

Funding This research did not receive any specific grant from funding agencies in the public, commercial, or not-for-profit sector.

Compliance with ethical standards

Conflict of interest The authors declare that they have no conflicts of interest.

Ethics approval This study was approved by the Institutional Review Board, Reference Number HS-16-00725. For this type of study formal consent is not required.

References

1. Agarwal AK, Jeyasingh P, Gupta SC, Gupta CD, Sahai A (1984) Peroneal tubercle and its variations in the Indian calcanei. Anat Anz 156:241–244
2. Boles MA, Lomasney LM, Demos TC, Sage RA (1997) Enlarged peroneal process with peroneus longus tendon entrapment. Skeletal Radiol 26:313–315
3. Buschmann WR, Cheung Y, Jahss MH (1991) Magnetic resonance imaging of anomalous leg muscles: accessory soleus, peroneus quartus and the flexor digitorum longus accessorius. Foot Ankle 12:109–116
4. Cho J, Kim JY, Song DG, Lee WC (2014) Comparison of outcome after retinaculum repair with and without fibular groove deepening for recurrent dislocation of the peroneal tendons. Foot Ankle Int 35:683–689. https://doi.org/10.1177/1071100714531233
5. Coskun N, Yuksel M, Cevener M, Arican RY, Ozdemir H, Bircan O, Sindel T, Ilgi S, Sindel M (2009) Incidence of accessory ossicles and sesamoid bones in the feet: a radiographic study of the Turkish subjects. Surg Radiol Anat 31:19–24. https://doi.org/10.1007/s00276-008-0383-9
6. Galli MM, Protzman NM, Mandelker EM, Malhotra AD, Schwartz E, Brigido SA (2015) An examination of anatomic variants and incidental peroneal tendon pathologic features: a comprehensive MRI review of asymptomatic lateral ankles. J Foot Ankle Surg 54:164–172. https://doi.org/10.1053/j.jfas.2014.11.005
7. Geller J, Lin S, Cordas D, Vieira P (2003) Relationship of a low-lying muscle belly to tears of the peroneus brevis tendon. Am J Orthop (Belle Mead NJ) 32:541–544
8. Hammerschlag WA, Goldner JL (1989) Chronic peroneal tendon subluxation produced by an anomalous peroneus brevis: case report and literature review. Foot Ankle 10:45–47
9. Highlander P, Pearson KT, Burns P (2015) Magnetic resonance imaging analysis of peroneal tendon pathology associated with low-lying peroneus brevis muscle belly: a case-control study. Foot Ankle Spec 8:347–353. https://doi.org/10.1177/1938640015569764
10. Kumai T, Benjamin M (2003) The histological structure of the malleolar groove of the fibula in man: its direct bearing on the displacement of peroneal tendons and their surgical repair. J Anat 203:257–262
11. Mirmiran R, Squire C, Wassell D (2015) Prevalence and Role of a low-lying peroneus brevis muscle belly in patients with peroneal tendon pathologic features: a potential source of tendon subluxation. J Foot Ankle Surg 54:872–875. https://doi.org/10.1053/j.jfas.2015.02.012
12. O'Neil JT, Pedowitz DI, Kerbel YE, Codding JL, Zoga AC, Raikin SM (2016) Peroneal tendon abnormalities on routine magnetic resonance imaging of the foot and ankle. Foot Ankle Int 37:743–747. https://doi.org/10.1177/1071100716635645
13. Oden RR (1987) Tendon injuries about the ankle resulting from skiing. Clin Orthop Relat Res:63–69
14. Ogawa BK, Thordarson DB (2007) Current concepts review: peroneal tendon subluxation and dislocation. Foot Ankle Int 28:1034–1040. https://doi.org/10.3113/FAI.2007.1034
15. Ozbag D, Gumusalan Y, Uzel M, Cetinus E (2008) Morphometrical features of the human malleolar groove. Foot Ankle Int 29:77–81. https://doi.org/10.3113/FAI.2008.0077
16. Rosenberg ZS, Bencardino J, Astion D, Schweitzer ME, Rokito A, Sheskier S (2003) MRI features of chronic injuries of the superior peroneal retinaculum. AJR Am J Roentgenol 181:1551–1557. https://doi.org/10.2214/ajr.181.6.1811551
17. Sarrafian SK (1993) Anatomy of the foot and ankle: descriptive, topographic, functional, 2nd edn. Lippincott, Philadelphia
18. Saupe N, Mengiardi B, Pfirrmann CW, Vienne P, Seifert B, Zanetti M (2007) Anatomic variants associated with peroneal tendon disorders: MR imaging findings in volunteers with asymptomatic ankles. Radiology 242:509–517. https://doi.org/10.1148/radiol.2422051993
19. Sobel M, Geppert MJ, Olson EJ, Bohne WH, Arnoczky SP (1992) The dynamics of peroneus brevis tendon splits: a proposed mechanism, technique of diagnosis, and classification of injury. Foot Ankle 13:413–422
20. Sookur PA, Naraghi AM, Bleakney RR, Jalan R, Chan O, White LM (2008) Accessory muscles: anatomy, symptoms, and radiologic evaluation. Radiographics 28:481–499. https://doi.org/10.1148/rg.282075064
21. Stockton KG, Brodsky JW (2014) Peroneus longus tears associated with pathology of the os peroneum. Foot Ankle Int 35:346–352. https://doi.org/10.1177/1071100714522026
22. Trevino S, Baumhauer JF (1992) Tendon injuries of the foot and ankle. Clin Sports Med 11:727–739
23. van Dijk PAD, Vopat BG, Guss D, Younger A, DiGiovanni CW (2017) Retromalleolar groove deepening in recurrent peroneal tendon dislocation: technique tip. Orthop J Sports Med 5:2325967117706673. https://doi.org/10.1177/2325967117706673

24. Vega J, Batista JP, Golano P, Dalmau A, Viladot R (2013) Tendoscopic groove deepening for chronic subluxation of the peroneal tendons. Foot Ankle Int 34:832–840. https://doi.org/10.1177/1071100713483098
25. Wang XT, Rosenberg ZS, Mechlin MB, Schweitzer ME (2005) Normal variants and diseases of the peroneal tendons and superior peroneal retinaculum: MR imaging features. Radiographics 25:587–602. https://doi.org/10.1148/rg.253045123
26. Zammit J, Singh D (2003) The peroneus quartus muscle. Anatomy and clinical relevance. J Bone Joint Surg Br 85:1134–1137